AN EXPERIMENTAL INVESTIGATION OF HIGH FREQUENCY COMBUSTION INSTABILITY IN A FUEL-AIR COMBUSTOR

Thesis by

Don E. Rogers

In Partial Fulfillment of the Requirements

For the Degree of

Aeronautical Engineer

California Institute of Technology

Pasadena, California

1954

ACKNOWLEDGMENTS

I wish to thank Dr. Frank E. Marble for initiating this problem and for his help and guidance throughout the investigation. I would also like to thank Dr. F. H. Wright and Mr. E. E. Zukoski for the numerous discussions of the problem which facilitated the study greatly.

In addition I would like to express my gratitude to the staff of the Jet Propulsion Laboratory of the California Institute of Technology where the experimental program was conducted. The assistance rendered by Mr. Clifford Reeser and Mr. George McFarland in the design and construction of the test equipment is gratefully acknowledged.

The excellent preparation of the manuscript is due to Mrs. Mabel Swafford whose efforts are greatly appreciated.

ABSTRACT

The results of an experimental investigation of high frequency combustion instability in a fuel-air combustor are described. The phenomenon is described in terms of alterations in the flame geometry and pressure changes associated with the flow field. Quantitative measurements of the pressure fluctuations are presented and the effects of various system parameters on the instability are indicated.

A possible mechanism for forcing and sustaining the oscillations as indicated by the experimental data is suggested and discussed.

TABLE OF CONTENTS

NOMENCLATURE

M = Average Mach Number

P_o = Inlet Total Pressure (Gage)

P_A = Atmospheric Pressure

ϕ = Equivalence Ratio

I. INTRODUCTION

High frequency combustion chamber oscillations have been observed in rocket motors for some time and more recently in ramjet combustion chambers and turbojet afterburners. This phenomenon differs greatly from rough burning in several respects. The sound emitted by a burner operating in this condition is a loud high-pitched screeching noise which has led to the general designation of screeching combustion. The process is further characterized by high frequency pressure pulsations which are clearly defined and exhibit none of the random characteristics associated with rough burning. The phenomenon further differs from other types of combustion instability in that it has no deleterious effects on the combustion process and does not lead to premature blowout.

This type of instability represents a serious difficulty in engine development work due to the rapid structural failures of the combustor and its components which result from even brief exposures to screeching operation. The particular items contributing most toward structural damage are the large increases in wall heat transfer coefficient which accompany the instability and the amplitudes of the associated pressure oscillations. The attendant increase in noise level which occurs with the onset of screech constitutes an additional undesirable feature.

The general features of screech in turbojet afterburners has been discussed by R. Newton and J. Truman[1] and by H. Wisniowski.[2] The former work indicates that screeching frequencies correspond to resonant modes of transverse oscillations in the burner duct similar to the situation which has been suggested for high frequency combustion instability in

liquid and solid propellant rocket motors by L. Crocco[3] and S. I. Cheng.[4] The problem has also been studied by R. Smith and D. Sprenger.[5] The priority in recognizing the importance of this unique phenomenon and some features of its mechanism must, however, be awarded to the Research Division of the United Aircraft Corporation. The criterion for exciting such resonant oscillations through heat addition has been discussed classically by Rayleigh,[6] and recently A. Putnam has extended the stability criterion in conjunction with the analysis of "organ pipe" modes of oscillation in burner ducts.[7] In these analyses however, the essential physical process whereby the heat must be released in certain phase relationship with the local pressure variations has not been demonstrated and consequently the mechanism of maintaining self-excited oscillations in a combustion system is incomplete. P. Blackshear,[8] working on this problem at the Lewis Laboratory of the N.A.C.A., has made the suggestion that the heat release is augmented by distortion of the flame front as the wave passes through it. The arrangement permits the generation of self-excited waves although the connection with the process taking place in ramjet combustion chambers and afterburners is not at all clear. Consequently an experimental investigation was undertaken utilizing a simulated flame holder and combustion chamber to clarify some features of the exciting or forcing mechanism of the high frequency instability. In spite of the fact that this model grossly simplifies the physical situation, it is felt that the significant features have been retained so that the mechanism is not seriously altered from that existing in conventional burners.

Initial results indicate that screech is accompanied by regular,

asymmetric shedding of vortices from the edges of the flame holder. The shedding occurs at a frequency which closely matches that of the pressure fluctuations. Data secured by optical techniques and direct pressure measurements are also presented to indicate the effects of Mach Number, equivalence ratio and inlet temperature on the amplitude and frequency of the screech oscillations. A definite mechanism for exciting screeching oscillations is suggested by the experimental evidence.

II. EQUIPMENT

The general features of the experimental apparatus used in this investigation are shown schematically in Figure 1. The study was conducted in an unthrottled, rectangular combustor with a constant cross-sectional area of 1 x 4 in^2. The combustor was equipped with a 70% blockage, solid wedge flame holder. Vycor glass windows were provided downstream of the flame holder to allow photographic studies.

Controlled and metered quantities of fuel and air were introduced into the combustor from a large plenum chamber by means of a converging nozzle which provided a contraction ratio of 28/1. Consequently the combustible mixture at the entrance to the combustion chamber was of uniform mixture strength, velocity and temperature, and of low turbulence level.

Air-Flow Control. Metered and regulated air for the combustor was supplied by a reciprocating compressor system at 64 p.s.i.g. with a capacity of 3.7 lbs/sec. The air mass flow rate was controlled by a sonic throat regulating valve installed upstream from both the fuel injector and the heat exchanger. The sonic throat in the regulating valve allowed operation at constant air mass flow despite variations in air temperature or fuel flow. The air mass flow rate was also unaffected by any pressure fluctuations in the combustion chamber by virtue of the sonic throat in the regulating valve.

Mixture Temperature Control. The metered air was heated in a conventional counter-flow, shell and tube type of heat exchanger and the air temperature was sensed and corrected by a commercial controller using a

gas filled sensing element. The sensing element was mounted in the air supply line upstream from the plenum chamber, and the controller positioned the butterfly valves that permitted more or less air to by-pass that heat exchanger as the heating demand was varied. Installation of the sensing element in the high velocity supply duct permitted rapid sensing of the mixture temperature and the use of a by-pass, flow control system eliminated the thermal inertia of the heat exchanger from the control cycle. The use of a proportional controller in conjunction with the previous factors allowed control of the mixture stagnation temperature in the plenum chamber within 5°F of the desired value despite variations in heating demand caused by changes in air or fuel-flow rate.

The entire hot-air ducting system was thermally insulated from the heat exchanger to the combustion chamber inlet to minimize heat losses and to stabilize the control process. The heating fluid supply for the heat exchanger was obtained from a turbojet can-type combustor. The physical appearance of the heating and air-metering system can be seen in Figure 2.

Plenum Chamber and Nozzle. The mixture plenum chamber was 12" in diameter and 5 feet in length. Six 150 mesh stainless steel screens were inserted just upstream of the nozzle to reduce the scale of the initially turbulent flow. Thin sheet metal blowout disks were also provided to relieve the pressure in the event of ignition of the mixture in the plenum chamber. The convergent nozzle faired smoothly from the 12 inch diameter of the plenum chamber to the 1 x 4 inch rectangular cross section of the combustion chamber in an axial distance of 18 inches. The photograph of

Figure 3 shows the appearance of the plenum chamber, nozzle and combustion chamber.

Combustion Chamber. The basic geometry of the experimental combustor is shown schematically in the drawing of Figure 4, and the photographs of Figures 5 and 6 show the details of the actual unit. The overall length of the combustor was 29 inches from inlet to exit and the apex of the wedge flame-holder was located $1\frac{1}{2}$ inches downstream of the inlet. The Vycor glass windows supplied a field of view of 4 x 5 inches of the region immediately downstream of the flame-holder.

Exploratory experiments with an uncooled combustion chamber of the same geometry established the desirability of adequate cooling. The high wall heat transfer rates associated with screech distorted the initial combustor to such a degree that pressure leakage, and window failures were severe problems. Consequently, water-cooling of the top, bottom, side-walls and flame holder was employed in the combustor used in this study. This feature allowed the use of pressure seals and eliminated the window failure problem. It further allowed extended periods of operation which in turn insured the achievement of thermal equilibrium prior to the recording of data.

The combustion chamber was fabricated of stainless steel to alleviate the corrosion problem arising from the water-cooling. The side walls of the burner were constructed of segmented plates, each of which was separately cooled and sealed. Since the plates were each 4 inches long in the axial direction, the design permitted variation of burner length in

increments of 4 inches. The separate side plates also facilitated the insertion of instrumentation and permitted measurements at various axial locations. The side plates were clamped to the combustor framework to allow rapid removal and installation.

The flame holder used throughout this investigation was a solid wedge with a semi-apex angle of 21° 50'. The area blockage of the flame holder was 70%. With an axial length of $3\frac{1}{2}$ inches it was constructed of stainless steel and equipped with an independent coolant circuit. The flame holder also served as part of the ignition system. A retractable probe entered the duct along the 4 inch dimension and carried the spark from a 10,000 volt transformer to the downstream side of the flame holder. The probe retracted after ignition to provide a smooth wall for the gas flow.

Fuel System. The fuel used in this investigation was a volatile liquid hydrocarbon blend used industrially as a paint thinner. It was chosen for the purpose because it was easily available, closely controlled in its production, easily metered as a liquid and because its chemical and thermodynamic properties allowed the use of available tables. The chemical and physical properties of the fuel are given in tabular form below.

FUEL SPECIFICATIONS*

Gravity (°API at 60°F)	61.4
Gravity, specific (60/60°F).	0.7335
Reid vapor pressure (lb)	4.0

* These specifications were obtained from an analysis made by the Union Oil Company at the request of the Jet Propulsion Laboratory.

Heat of combustion (Btu/lb)	
Gross	20,130
Net	18,793
ASTM distillation	
Initial (°F)	160
Maximum (°F)	220
Acid solubility (%)	7.0
Bromine number	0.003
Percentage of carbon	85.69
Percentage of hydrogen	14.23
Proximate analysis:	
Cyclopentane	1
Isohexane	14
n-Hexane	15
Methylcyclopentane	10
Cyclohexane	17
Benzene	2
Isoheptanes	14
n-Heptane	12
Methylcyclohexane	8
Toluene	3
C_8 paraffins	3
Ethylbenzene, Xylenes	1
	100

The fuel was supplied from a pressurized reservoir metered with calibrated rotameters and injected into the heated air stream about 40

feet upstream of the plenum chamber. The long length of piping involved provided adequate time for vaporization and mixing of the fuel with the air stream before the plenum chamber was reached. Installation of the temperature control sensing element downstream of the fuel injection point allowed the temperature controller to compensate for the mixture temperature variations which would otherwise result from the vaporization requirements of the fuel as the mixture ratio was varied.

Instrumentation. The following measurements were made to determine the basic parameters of the investigation.

(1) Fuel rate was measured by 10" flowrators which were calibrated on the fuel used.

(2) Plenum chamber total temperature was established by a calibrated iron-constantan thermocouple.

(3) Plenum chamber total pressure was measured with a mercury manometer.

(4) Combustion chamber inlet static pressure was determined with a water-filled differential manometer.

(5) Air rate was measured by means of a sharp-edge orifice installed upstream of the heat exchanger. The installation of the orifice and the associated pressure measurements were made in accordance with standard ASME practice for such devices.

Direct measurement of the frequency and amplitude of the pressure fluctuations were obtained by means of Photocon capacitance-type gages flush-mounted in the side wall of the combustion chamber. These gages were water-cooled with a maximum rating of 100 p.s.i.g. and a natural

frequency of 75,000 cps. The output of each gage was observed on a Dumont dual beam oscilliscope and recorded with a Land-Polaroid camera.

Optical studies were conducted with a single-pass, double mirror schlieren system of conventional arrangement. Light for the system was provided by a General Electric mercury vapor lamp which could be driven continuously for high speed moving pictures or flashed for instantaneous pictures. High speed moving pictures were secured with a Western Electric Fastax camera operated at its maximum speed of 7000 frames per second. A timing pulse was inserted on the film to allow accurate determination of the framing rate.

III. EXPERIMENTAL DATA AND RESULTS

The initial portion of the experimental program was devoted largely to exploring the general gross features of the instability. Following this exploratory investigation into the nature of screeching combustion, a systematic variation of some of the principal parameters was undertaken with the objective of determining the basic mechanism sustaining the oscillations. The resulting data were then examined and a particular mechanism suggested, as indicated by the experimental evidence.

Description of the Phenomenon. The distortion of the flame front which occurs with the onset of screech is one of the most striking features of the phenomenon. The direct photographs of Figures 7 and 8 illustrate the changes in the flame envelope which occur with transition to screeching operation. Figure 7 was taken during smooth burning while Figure 8 was taken shortly after the onset of screech. The screeching operation of Figure 8 was secured by a 1% increase in fuel flow rate above the value corresponding to Figure 7.

The wave-shaped contour of the flame boundary suggested the presence of a standing longitudinal wave in the burner. However further investigation with flash schlieren photographs eliminated this possibility. Comparative flash schlieren photographs of smooth and screeching combustion are shown in Figures 9 and 10. These pictures were obtained at the same operating conditions as those of Figures 7 and 8 and clearly show the presence of vortices downstream of the flame holder. Figures 9 and 10 also indicate the asymmetric nature of the shedding and measurements made

from a sequence of twelve pictures taken at the same operating conditions substantiated the regularity of the phenomenon. The appearance of the vortex arrangement at various times is indicated by the pictures of Figure 11 which were selected from the previously mentioned sequence. The sequence of photographs further indicated that the vortices are shed 180° out of phase with respect to the downstream face of the flame holder.

The schlieren photographs of Figures 9 through 11 were taken with the knife edge installed vertically and consequently delineate only streamwise density gradients. This was done to minimize the effects of the hot Vycor window which introduced large transverse gradients. The flash duration of the BH-6 lamp used as a light source was too long to completely stop the motion and as a result the photographs show a marked streaking in the high velocity regions. The geometry of the optical system used to secure these pictures was such that the white regions in the photographs represent areas in which the temperatures are lower comparatively than in the black regions. The horizontal black line apparent in all of the schlieren photographs is due to a crack in one of the windows which was small enough to allow continued operation.

Some further characteristics of the phenomenon are best displayed by the plot of Figure 12. This figure depicts the variation of combustion chamber gage inlet total pressure with fuel-air ratio for constant mass flow and inlet total temperature. The values of the gage inlet total pressure are presented in dimensionless form as the ratio of the gage inlet total pressure to the absolute inlet total pressure. The fuel-air ratio is normalized by division by the stoichiometric value and referred

to as the equivalence ratio, ϕ. Values of $\phi < 1.0$ therefore indicate mixtures with excess air and values of $\phi > 1.0$ indicate mixtures with excess fuel. The mass flow is not precisely constant for this figure due to the increased fuel rate required to raise the equivalence ratio. The change in the total mass flow is small, however, amounting to an increase of 4% in changing the equivalence ratio from 0.80 to 1.40.

Since the combustion chamber is unthrottled at the exit and the mass flow is essentially constant for Figure 12, the increase in the inlet total pressure must arise largely from an increase in the momentum pressure drop through the combustor associated with the release of heat in a flowing gas. This is reasonable in view of the fact that the frictional pressure drop should vary only slightly with ϕ. It can be seen from the figure that a sudden jump in the inlet total pressure occurs in the vicinity of $\phi = 1.025$. This is the point at which transition to screeching operation occurs as the fuel flow is increased. Since the heat release curve is continuous as a function of equivalence ratio, the discontinuous increase in the total pressure must correspond to a comparable rise in the heat release. Since higher heat release occurs during screeching combustion than smooth combustion, this must be attributable to an increase in the combustion efficiency.

The equivalence ratio at which this increase occurs is reproducible within 1% of the fuel flow for a given set of inlet conditions. The value of the equivalence ratio which first produces screeching operation for increasing fuel flow is hereafter referred to as the lean screech limit. As the data of Figure 12 indicates, a different value exists when the

equivalence ratio is decreased. The direction of the variations in equivalence ratio followed in defining the hysteresis loop are indicated by arrows on Figure 12. Sufficient time was spent at each point to insure achievement of thermal equilibrium and the coolant rate through the combustor was maintained constant during the operation. The operating range of the experimental combustion chamber was bounded at low equivalence ratio by a conventional lean blowout during smooth combustion. The rich blowout limit was found to occur during screeching operation by means of a violent large amplitude instability which was rather random in nature.

An investigation of the nature of the pressure oscillations accompanying screeching combustion furnished further information. Quantitative data on the frequency and amplitude of the pressure oscillations were obtained by installing the water-cooled pressure pick-up of the type described in Section II, 11 inches downstream of the rear face of the flame holder. The gage was flush-mounted on the centerline of the 4 inch dimension of the duct and consequently sensed variations in static pressure. A static calibration was made to allow determination of the peak-to-peak amplitude of the oscillations. The output trace was regular enough to allow observation on a dual beam oscilliscope. A time trace from a calibrated signal generator was fed into the other beam of the oscilliscope to permit determination of the frequency of the pulsations.

The independent variable for this portion of the program was again the equivalence ratio. The pressure traces shown in Figure 13 were obtained at constant mass flow and inlet total temperature and the corresponding values of ϕ for each trace are shown on the figure. The time

base in all cases is 1/1000 sec. peak-to-peak. The transition to screeching operation is clearly demonstrated by the appearance of the high frequency oscillation. It can also be seen that the low frequency oscillation is present even during smooth burning but undergoes an increase in amplitude with the onset of screech. The low frequency component was established as being about 285 cycles/sec whereas the high frequency screech component was a 3800 cycle oscillation. No appreciable variation of frequency with equivalence ratio was found for either the high or low frequency components.

The amplitudes as determined from the data of Figure 13 are shown plotted as a function of equivalence ratio in Figure 14. The ordinate of the plot represents the peak-to-peak amplitude of a particular component of the oscillation expressed as a percentage of the inlet total pressure. This figure demonstrates the sudden appearance of the high frequency component with the onset of screech and also emphasizes the discontinuous increase in amplitude of the low frequency component which occurs simultaneously. Figure 14 also affords an interesting comparison of the effect of equivalence ratio on the relative amplitudes of the high and low frequency oscillation. The amplitude of the low frequency fluctuation appears to diminish somewhat with increasing equivalence ratio in the screech region. The amplitude of the high-frequency screech component, however displays a continuous increase with equivalence ratio up to the point where blowout occurred due to the previously mentioned rich instability limit. It should be noted that due to the characteristics of the experimental apparatus, the burner inlet pressure rises with increasing equivalence ratio (see Fig. 12).

An investigation of the wave-shaped flame boundary which characterized screeching operation necessitated securing high-speed schlieren moving pictures. The primary objective was to determine the manner in which the vortices, revealed by the flash pictures, could produce a wave-shaped flame envelope the contour of which was fixed in space. The film strips reproduced in Figure 15 are representative of a portion of the data. For the photographs shown the knife-edge was again vertical to emphasize streamwise gradients and the comparative temperature relationship between light and dark regions is as discussed previously. The camera was operated at its maximum speed of 7000 frames per second and a 1/1000 second timing pulse was inserted on the film to allow computation of the framing rate.

Examination of the films indicated that as the camera was accelerating up to the maximum speed of 7000 frames per second a stroboscopic effect was secured when the framing rate of the camera equalled the shedding rate of the vortices. Film strip A of Figure 15, which was taken at 4100 frames per second, illustrates this effect and attests to the regularity of the phenomenon. Film strip B indicates the appearance of the vortex shedding at the maximum camera speed of 7000 frames per second.

A study of the film data in the stroboscopic region and in the high speed region indicated that the flame front associated with each lip of the flame holder was undergoing a transverse oscillation bearing a fixed phase relation to the vortex shedding from each lip. As a consequence of this transverse movement of the flame front, each vortex shed from one lip followed the same sinusoidal path while moving downstream. Because of this extreme regularity, the wavy path traced by successive vortices

defined to the eye the flame envelope described earlier. A rough calculation of the frequency of the first unsymmetrical transverse mode of gas oscillation indicates a substantial check of the pulsation frequency observed.

Effects of Various Parameters. The effect of the gas velocity on screeching combustion was initially noticed by visual observation of the flame boundaries. It was observed that as the mixture velocity was increased the wave-length of the flame envelope deformation also increased. The high speed schlieren photographs of Figure 16 depict the effect of gas velocity on the vortex formation. The local velocity which appeared to be most significant in these studies is that just prior to separation from the flame holder, since it characterizes the region in which the vortices are first formed. Due to boundary layer growth as well as local acceleration over the flame holder, the velocity profile at the downstream edge of the flame holder is non-uniform. Consequently where Mach Number is specified as the independent variable, it was taken as the average value, determined from the mass flow, inlet total pressure and inlet total temperature using the conventional one-dimensional gas dynamics. The values of the average Mach Number associated with each film strip are indicated on the figure.

The amplitude of the pressure oscillations associated with this periodic flame field was obtained, as outlined previously, with a flush mounted pressure pick-up located 11 inches downstream of the flame holder. The results of these measurements, shown in Figure 17, represent the peak-to-peak amplitude of a particular component expressed as a percentage of

the inlet total pressure. The relative insensitivity of the absolute amplitude of the high and low frequency oscillations to the variation in inlet dynamic pressure indicate that the dynamic pressure itself makes little contribution to the magnitude of the pressure fluctuation in this Mach Number range. Consequently the excitation of the pressure pulsations must arise largely from periodic variations in the burning rate. However it was observed that high values of the average Mach Number had a decided tendency to inhibit or prevent screech. At sufficiently high Mach Numbers, that is of the order of 0.70, the combustor screeched only intermittently and in a random fashion. As the Mach Number was further increased, a point was reached where it was not possible to initiate screech at all and the combustor burned smoothly over its operating range. This indicates that there exists a region, $0.55 < M < .070$, where an as yet unexplainable influence of the flow field takes place.

The associated frequencies were also determined and are presented as a function of the average Mach Number in Figure 18. The low frequency oscillation remained constant over the Mach Number range investigated and the screech frequency showed a slight decline with increasing Mach Number.

The previously discussed high speed schlieren moving pictures furnished a method of determining the effect of Mach Number on the vortex shedding rate. The shedding rate was ascertained by computing the camera framing speed at the stroboscopic point on the film which stopped all downstream motion of the vortices. The data of Figure 19 were obtained from a series of films taken at different values of the average Mach Number while maintaining constant values of equivalence ratio and inlet total temperature.

The shedding rate appears to decrease slightly with increasing Mach Number. The relative insensitivity of the vortex shedding rate to the Mach Number increase would indicate that this phenomenon is not related to the development of a Karman vortex street. The frequencies of Figure 18 are replotted on Figure 19 to allow a comparison of the values obtained from the pressure fluctuations with those secured by observation of the vortex shedding rate. The data agree well both in magnitude and functional variation but display a slight disparity at the lower Mach Number end of the curve. The data of Figures 18 and 19 establish a direct relationship between the vortex shedding mechanism and the high frequency pressure oscillations downstream of the flame holder.

A further effect of the average Mach Number was secured by examining its influence upon the equivalence ratio at which screech was first initiated. The equivalence ratio of the lean screech limit as a function of average Mach Number is shown in Figure 20. The data were obtained at constant inlet total temperature by increasing the fuel flow rate. As the curve of Figure 19 indicates, the critical equivalence ratio is not very sensitive to Mach Number variation and displays a tendency to approach the stoichiometric value as the average Mach Number is increased.

Figure 21 depicts the variation of vortex shedding rate with equivalence ratio, as determined from high speed schlieren moving pictures for a fixed mass flow and inlet total temperature. The data indicate a weak dependence of the shedding rate on the equivalence ratio. Frequency values secured with a flush-mounted pressure pick-up located 11 inches downstream of the flame holder are also included on Figure 21. Although the inlet

conditions are not the same for the two curves, the comparison again emphasizes the identity between the frequencies of the shedding rate and the measured pressure oscillations.

It was observed in the initial phases of this investigation that the inlet mixture temperature appeared to have a strong effect upon the value of the equivalence ratio at which screech occurred. The plot of Figure 22 presents the variation in the equivalence ratio at which transition to screeching operation occurred as a function of the inlet mixture temperature. These data were obtained during operation at constant mass flow by increasing the fuel rate to define the lean screech limit. The strong dependence of the lean screech limit on the mixture temperature is emphasized by comparison with the curve defining the lean blowout limit of the burner. The lean blowout limit of the burner was determined for a given inlet temperature by decreasing the fuel rate until the mixture ratio was too lean to sustain combustion. The equivalence ratio defining the lean blowout limit remains essentially constant over the temperature range investigated while the equivalence ratio defining the lean screech limit exhibits a decrease of some 25% over the same temperature range. The sensitivity of the phenomenon to the inlet mixture temperature suggests the presence of an ignition time lag factor in the mechanism producing the oscillations. This possibility appears reasonable in view of the fact that the mixture enthalpy increases arising from the inlet temperature increases are small when compared to the enthalpy changes associated with the variations in equivalence ratio.

The frequencies characterizing the oscillations encountered in this

combustor are clearly identified with a low frequency component in the vicinity of 285 cycles/sec and a high frequency component in the vicinity of 3800 cycles/sec. The low frequency component suggested the presence of a longitudinal oscillation between the flame holder and the burner exit. Since the frequencies characteristic of this type of an oscillation depend upon the burner length downstream of the flame holder, a series of frequency measurements were made with varying downstream burner lengths. The results of these tests indicated that the low frequency oscillation varied inversely with the amount of ducting downstream of the flame holder as would be expected for an axial oscillation. The high frequency component was unaffected however by changes in burner length. It was also observed that the burner would not screech under any conditions with less than $16\frac{1}{2}$ inches of ducting downstream of the flame holder.

IV. THE MECHANISM OF SCREECHING INSTABILITY

The foregoing experimental results provide certain crucial information upon which a tentative mechanism of screeching instability may be based. Referring to the specific burner, it is clear that the screech frequency is associated with the first (unsymmetrical) mode of transverse oscillation across the burner passage. The vortex shedding occurs at a frequency which is essentially that of the transverse oscillations and in such a fashion that the vortex shedding from one lip of the flame holder bears a definite and fixed phase relationship to the transverse movement of the gas. It appears, furthermore, that the energy exciting the pulsation is derived largely from a nonsteady and nonuniform combustion process rather than from the kinetic energy of gas flow over the flame holder lip.

Recent work[9] on the mechanism of flame stabilization has clarified the fact that flames are stabilized behind bluff bodies principally through the action of a relatively stable hot wake of combustion products. A portion of the fresh gas flowing about the body enters the wake recirculation zone by means of turbulent mixing and burns. This action supplies the heat required to maintain the wake temperature and to promote the formation of a stable flame which will propagate downstream. The source of high frequency pressure oscillations must, therefore, arise from the periodic transport of fresh combustible gas into the hot recirculation zone. It is proposed that this periodic transport process is accomplished by the vortices formed at the flame holder lip which consist largely of combustible material collected from the boundary layer built up on the

forward portion of the flame holder.

Consider, then, that such a pressure disturbance occurs near one lip of the flame holder. The resulting pressure wave propagates toward both walls of the duct, is reflected, and in the process disturbs the flow entering the channel at the other lip. This disturbance generates, in general, a vortex formation of combustible material which at the proper phase of the gas motion, moves into the hot recirculation zone. After an appropriate delay time associated with mixing and ignition, this material burns, forming a pressure disturbance similar to the original one but at the opposite lip. If the period of this transverse oscillation and the ignition delay time are in the appropriate relation, the amplitude of the oscillations will increase and the motion is unstable.

This mechanism is in agreement with the foregoing experimental results with the exception that it offers no explanation for the fact that the rich and lean screech limits are of a distinctly different nature. There appears no difficulty, however, in submitting the proposed mechanism to some critical tests to determine its validity. One such critical experiment would be to saturate the flame holder boundary layer with noncombustible material and observe the action in suppressing screech. The dependence of the suggested mechanism on a proper combustion time lag could be checked by utilizing different fuels with the same burner geometry.

The important feature of the mechanism is the relationship of a natural oscillation with a process of feeding combustible material into the recirculation region. It is quite possible, for example, that a symmetric mode could be excited in the same manner. This appears to be the case in axially symmetric burners.

V. SUMMARY OF RESULTS

As a consequence of the studies performed in the 1 x 4 in^2 experimental combustor, the following results were established regarding the observed high frequency instability:

Screeching operation was characterized by the onset of a 3800 cycle pressure oscillation which was not present during smooth burning. Screeching combustion was further characterized by a regular, asymmetric shedding of vortices from the flame holder lips. The flame front just downstream of the flame holder undergoes a transverse oscillation which bears a fixed phase relationship with the vortex shedding process. The frequency of the vortex shedding was established as matching that of the pressure oscillations and is compatible with the value associated with the first (asymmetrical) mode of transverse oscillations.

The amplitude of the pressure oscillations is relatively insensitive to the kinetic energy of the gas stream over the Mach Number range investigated. A nonsteady, nonuniform combustion process appears to establish the amplitude of the oscillations as indicated by the experimental data.

Combustion efficiency was observed to undergo a marked increase with transition from smooth to screeching combustion. Inlet mixture temperature was established as having a strong effect on the equivalence ratio of the lean screech limit. Variations in downstream burner length produced no measurable effect on the frequency of the screech oscillation.

A forcing mechanism for the oscillations, as indicated by the experimental data, is suggested and discussed. The basis of the mechanism is the phase relationship between a natural mode of oscillation and a process of furnishing fresh combustible material to the recirculation zone.

REFERENCES

1. Newton, R. T. and Truman, J. C., "An Approach to the Problem of Screech in Ducted Burners," Transactions ASME (To be Published).

2. Wisniowski, H. U., "Preliminary Experimental Investigation of Howling in Reheat Combustion Chambers," Laboratory Report LR-84. Ottawa (Canada): National Aeronautical Establishment, September, 1953.

3. Crocco, L., "Combustion Instability in Liquid Rocket Motors," Journal of the American Rocket Society, Part I, 21 (No. 6), 1951 and Part II, 22 (No. 1), 1952.

4. Cheng, S. I., "High Frequency Combustion Instability in Solid Propellant Rockets," Journal of the American Rocket Society, Part I, 24 (No. 1), 1954 and Part II, 24 (No. 2), 1954.

5. Smith, R. P. and Sprenger, D. F., "Combustion Instability in Solid Propellant Rockets," Fourth (International) Symposium on Combustion, 893-906. Baltimore: Williams and Wilkins Co.

6. Rayleigh, J. W. S., "Theory of Sound," New York: Dover Publ., 1945.

7. Putnam, A. A. and Dennis, W. R., "A Study of Burner Oscillations of the Organ-Pipe Type," Transactions ASME, 75:15, 1953.

8. Blackshear, P. L., "Driving Standing Waves by Heat Addition," Technical Memorandum No. 2772. Cleveland: National Advisory Committee for Aeronautics, 1952.

9. Zukoski, E. E., "Flame Stabilization on Bluff Bodies at Low and Intermediate Reynolds Numbers," (Doctoral Thesis in Aeronautical Engineering). Pasadena: California Institute of Technology, June, 1954

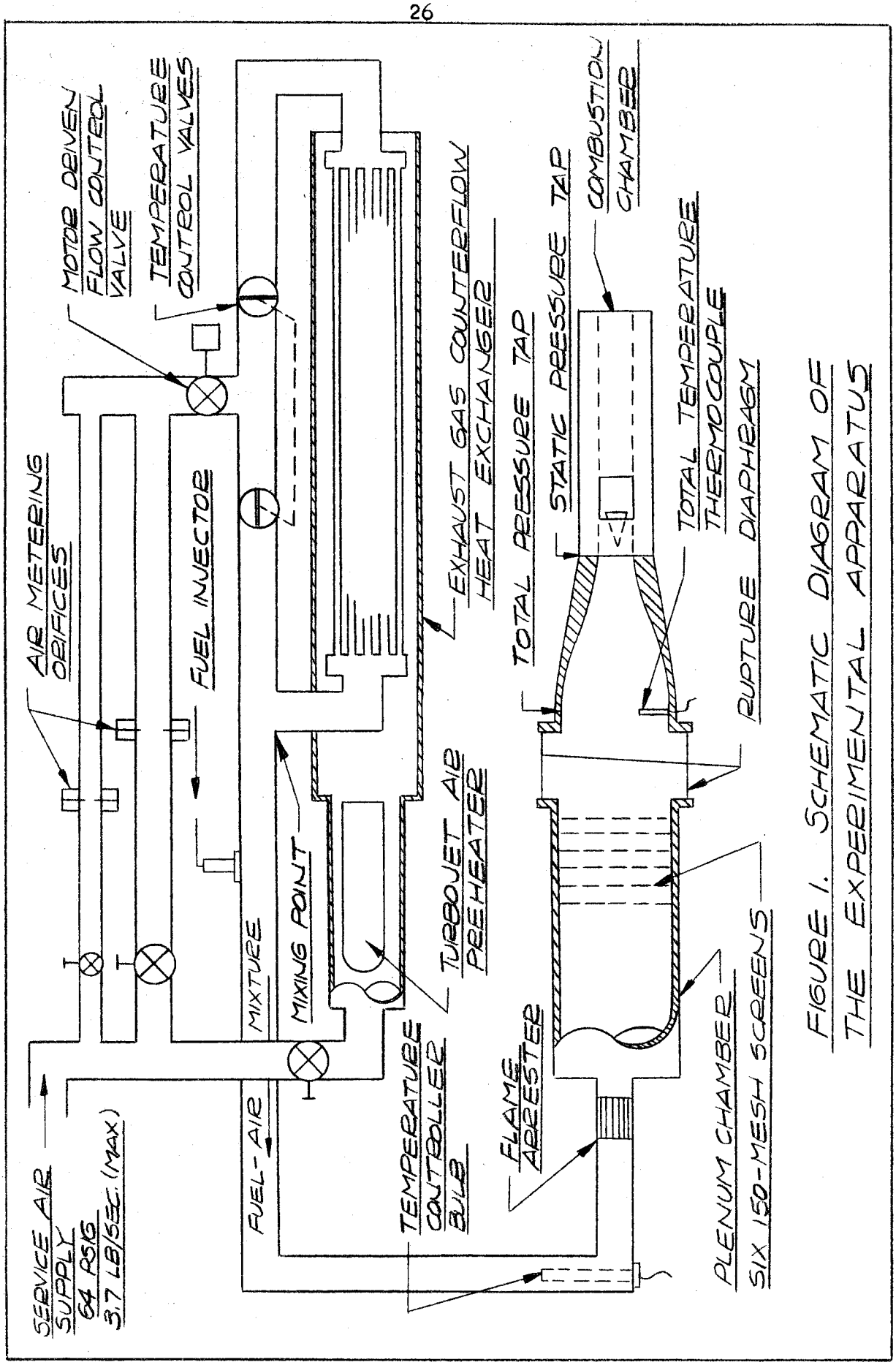

FIGURE 1. SCHEMATIC DIAGRAM OF THE EXPERIMENTAL APPARATUS

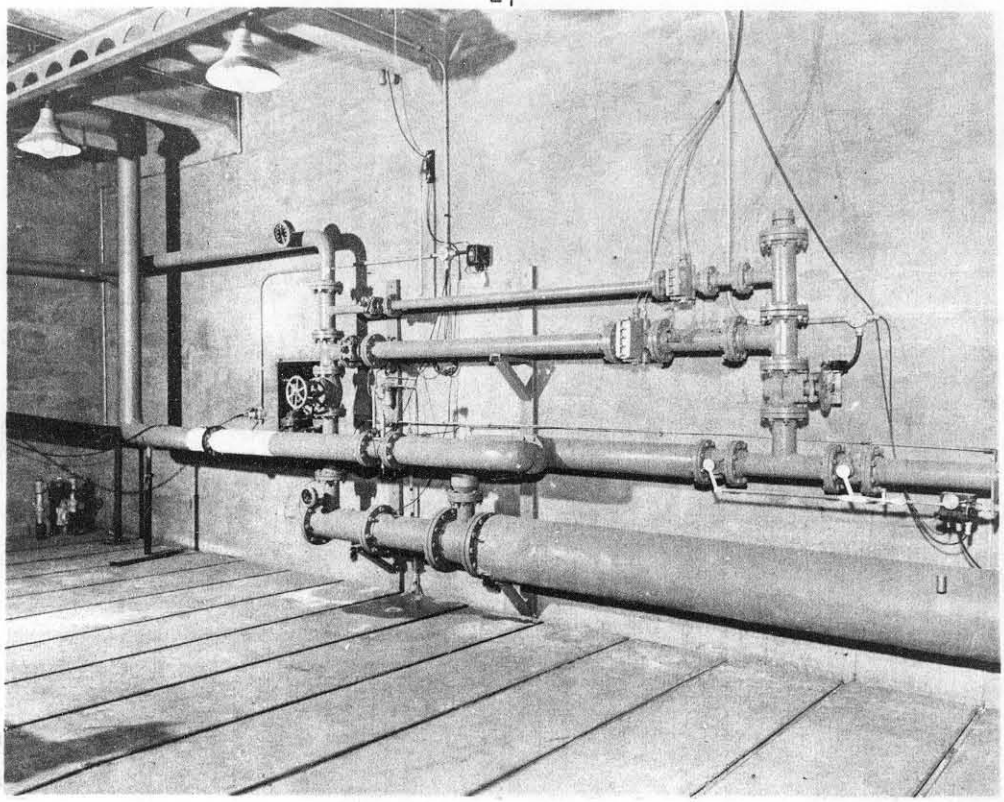

FIGURE 2. VIEW OF THE HEATING AND AIR METERING SYSTEMS

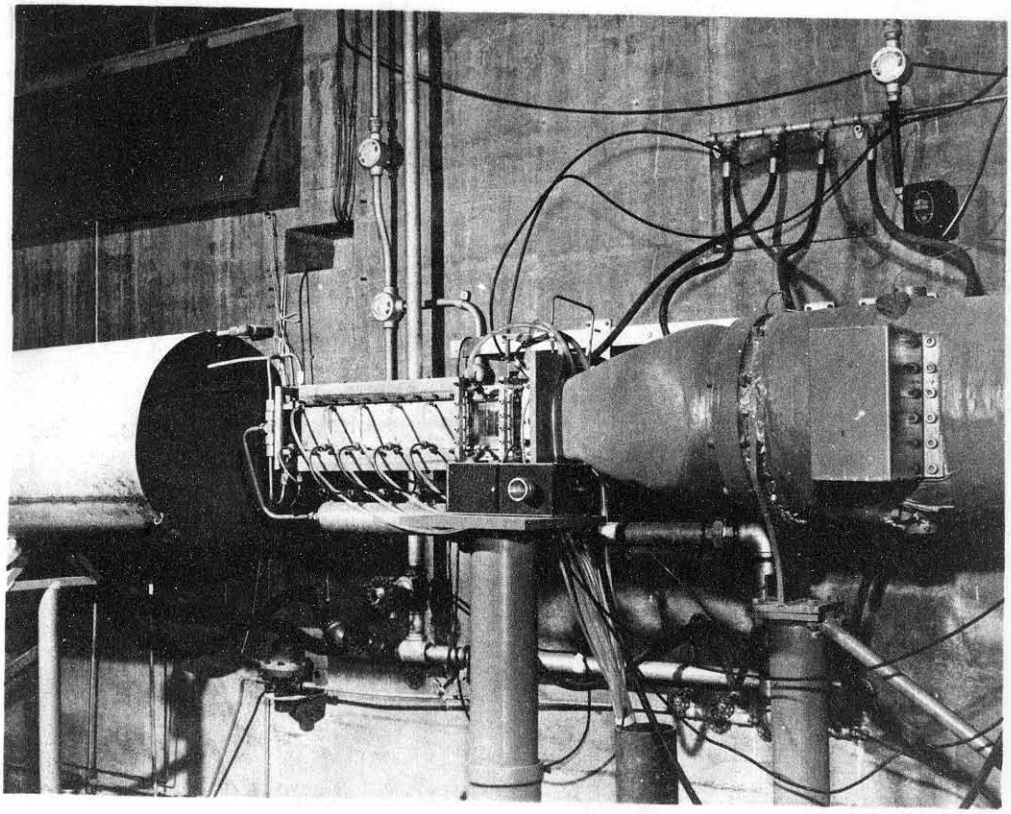

FIGURE 3. VIEW OF THE PLENUM CHAMBER AND NOZZLE

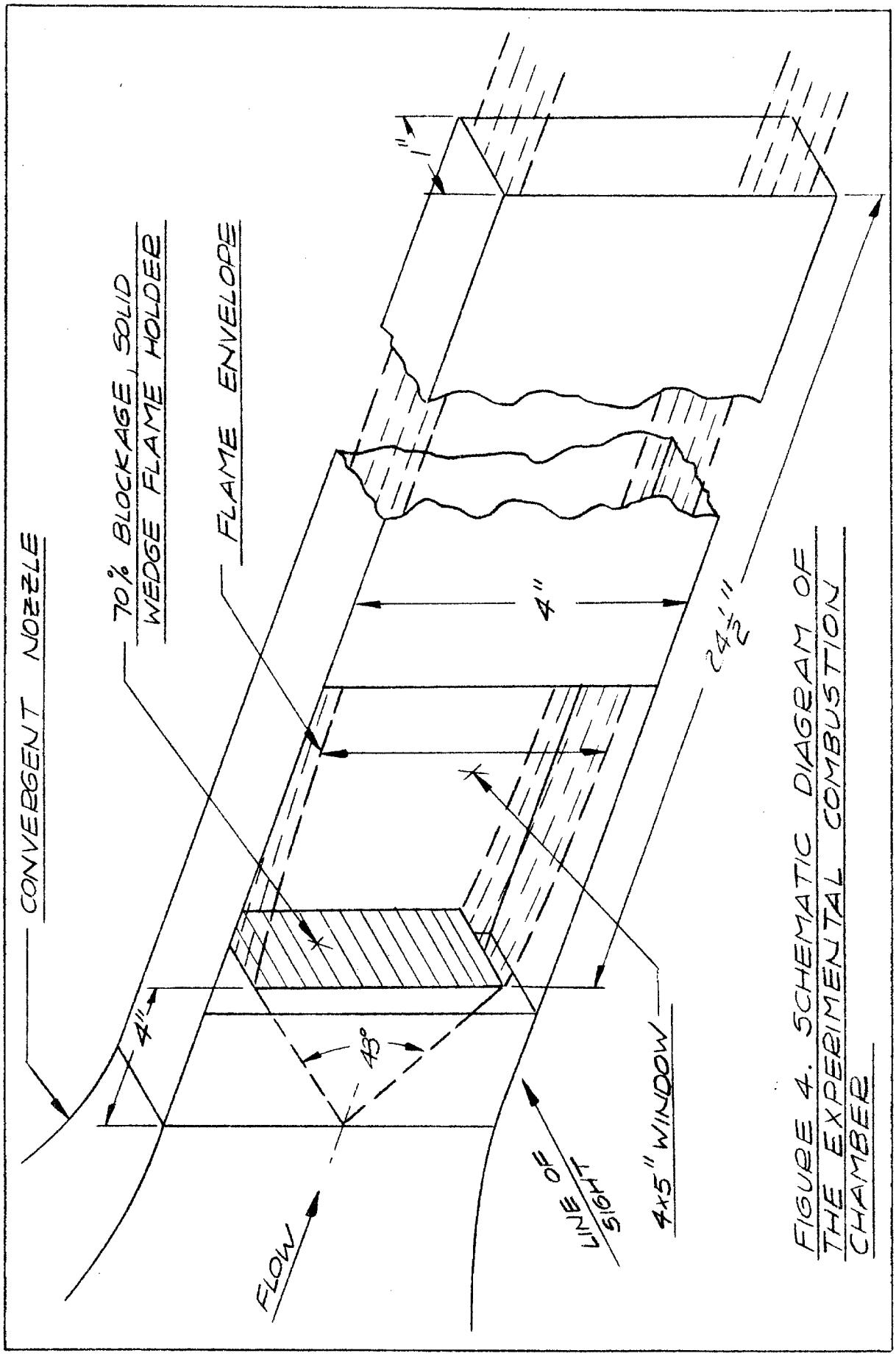

FIGURE 4. SCHEMATIC DIAGRAM OF THE EXPERIMENTAL COMBUSTION CHAMBER

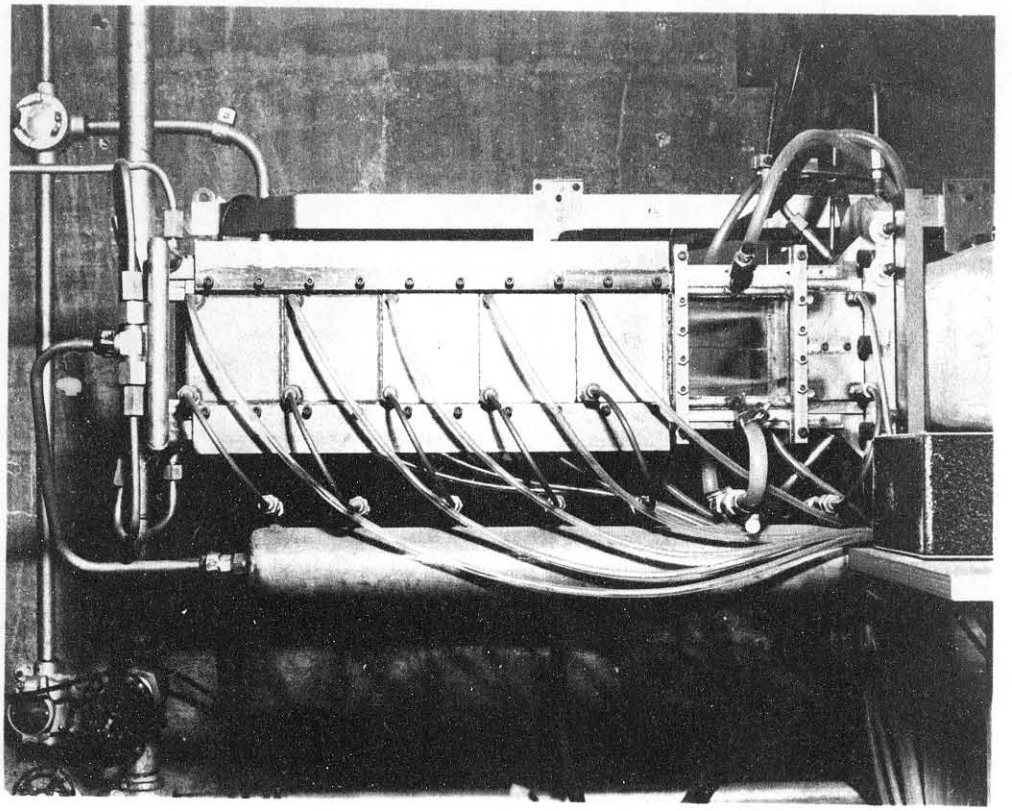

FIGURE 5. SIDE VIEW OF THE COMBUSTION CHAMBER

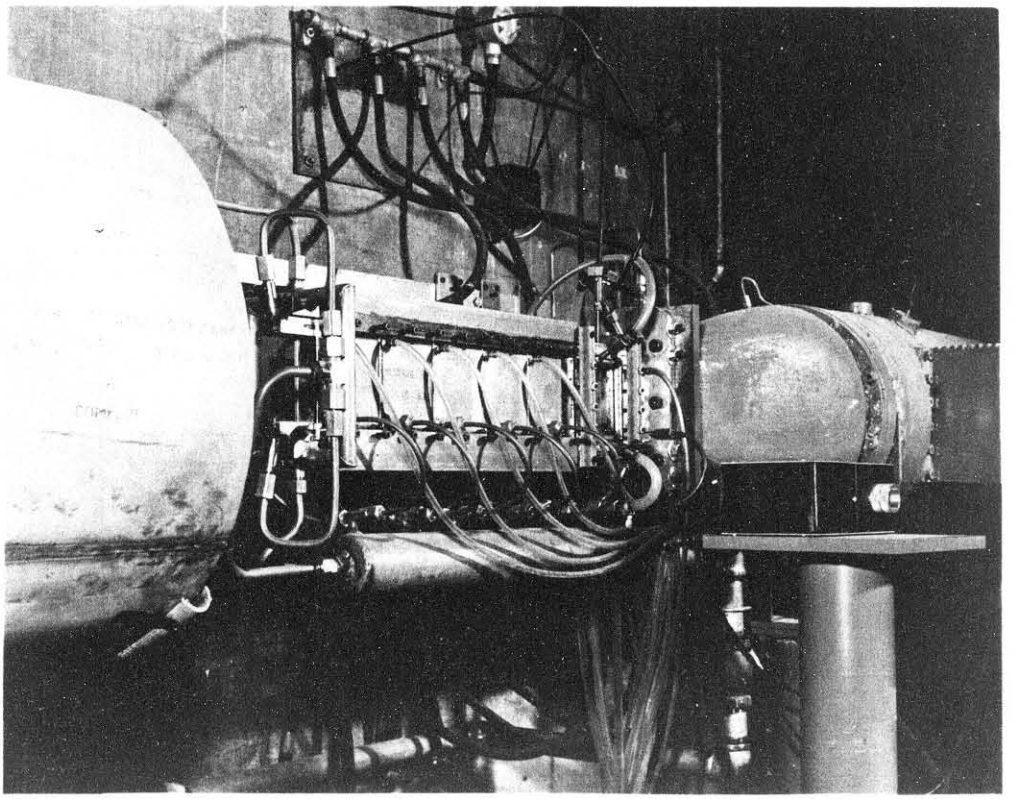

FIGURE 6. FRONT VIEW OF THE COMBUSTION CHAMBER

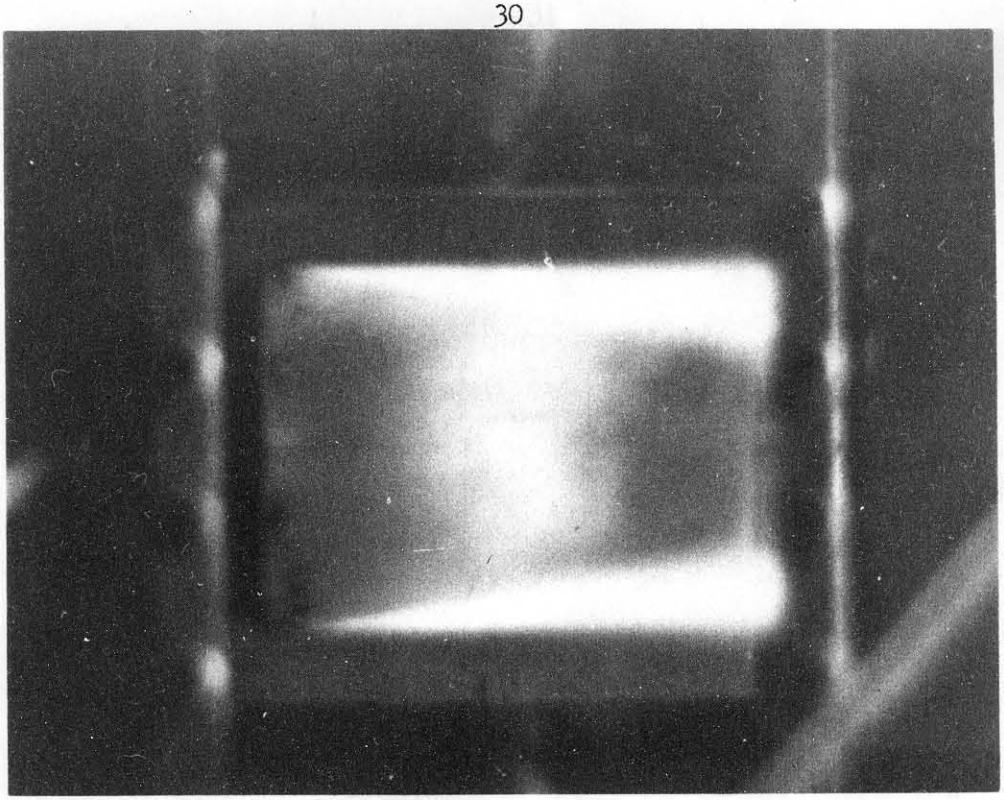

FIGURE 7. DIRECT PHOTOGRAPH OF SMOOTH COMBUSTION

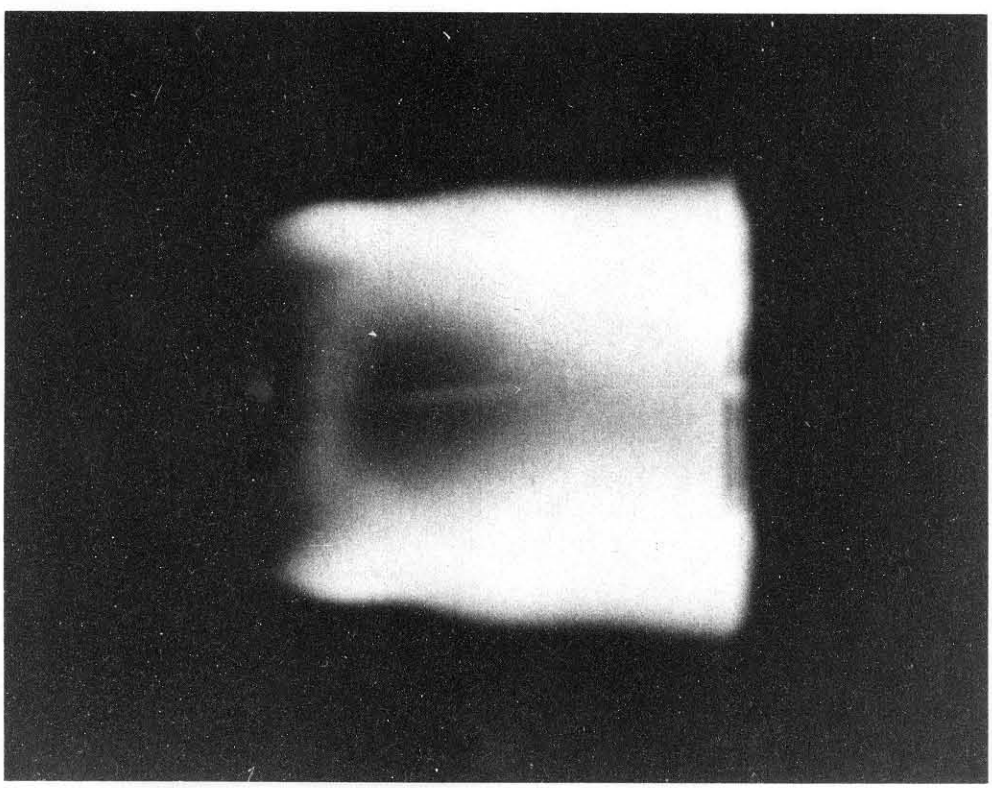

FIGURE 8. DIRECT PHOTOGRAPH OF SCREECHING COMBUSTION

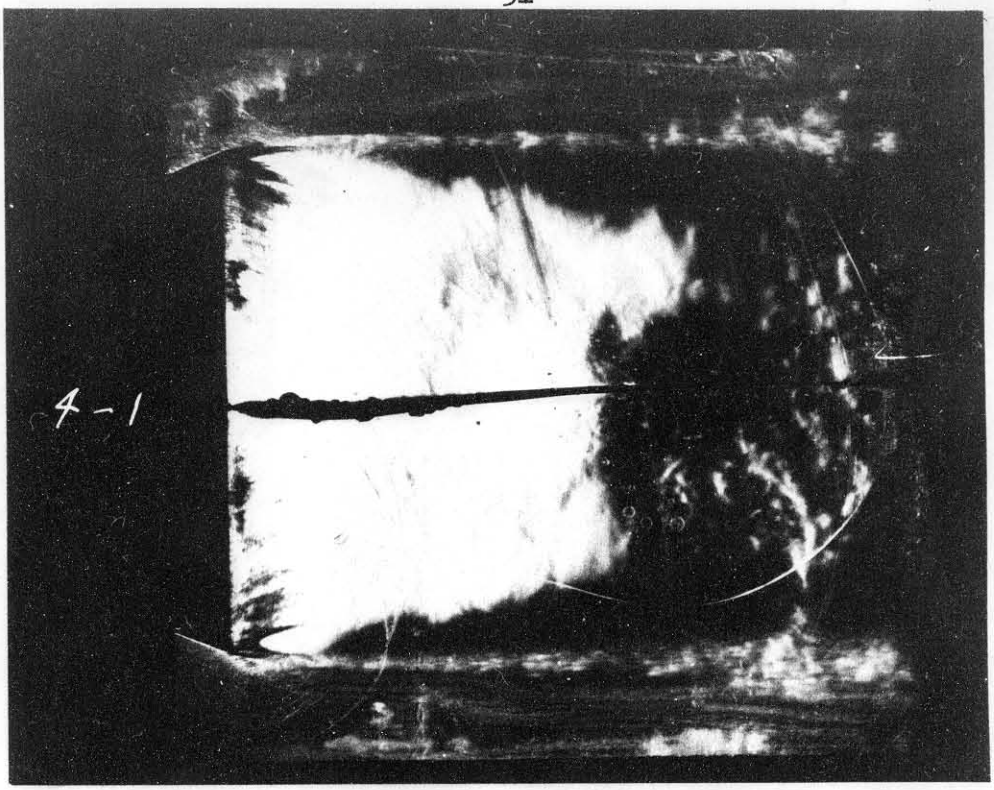

FIGURE 9. SCHLIEREN PHOTOGRAPH OF SMOOTH COMBUSTION

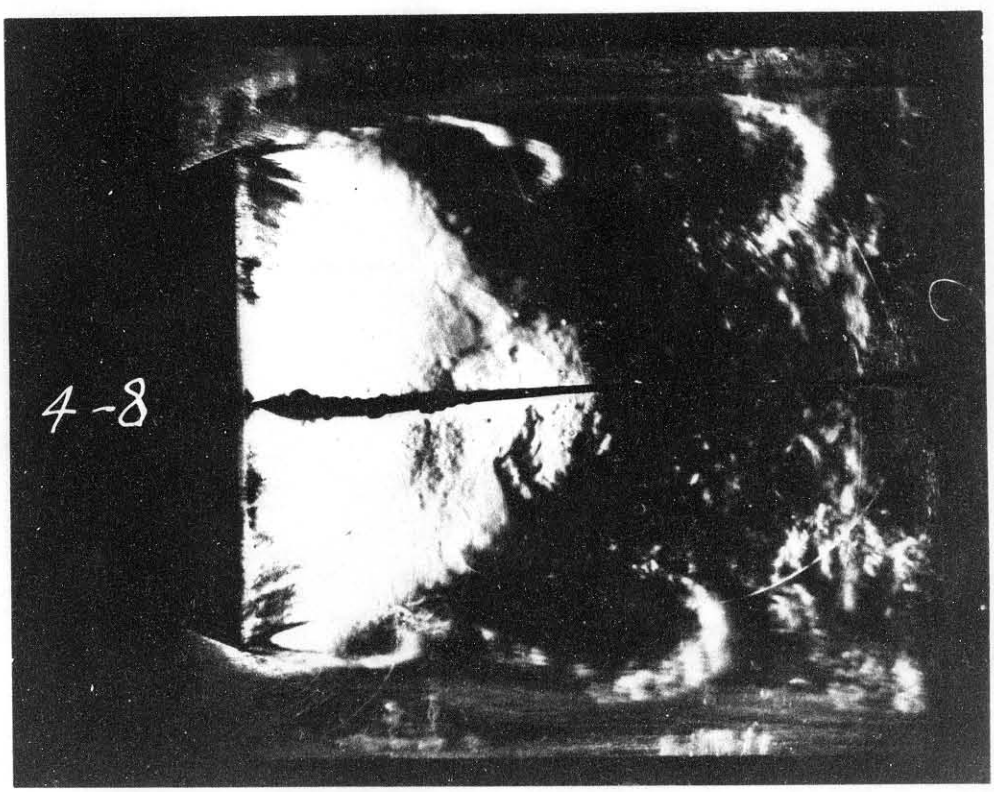

FIGURE 10. SCHLIEREN PHOTOGRAPH OF SCREECHING COMBUSTION

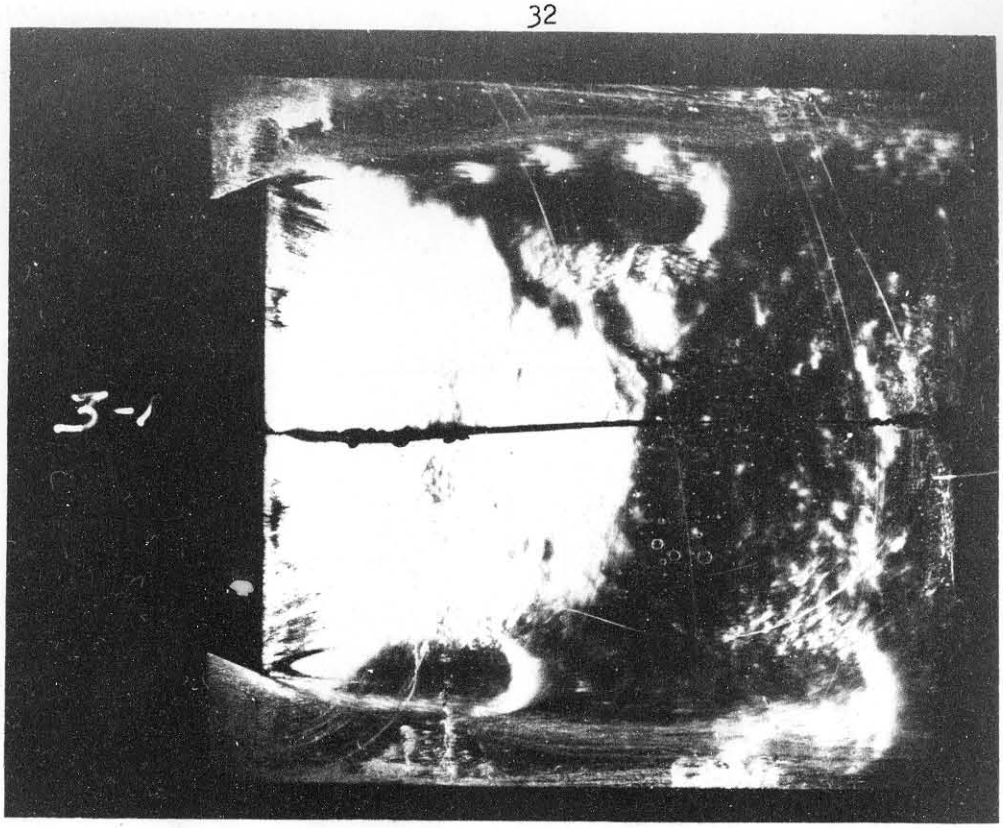

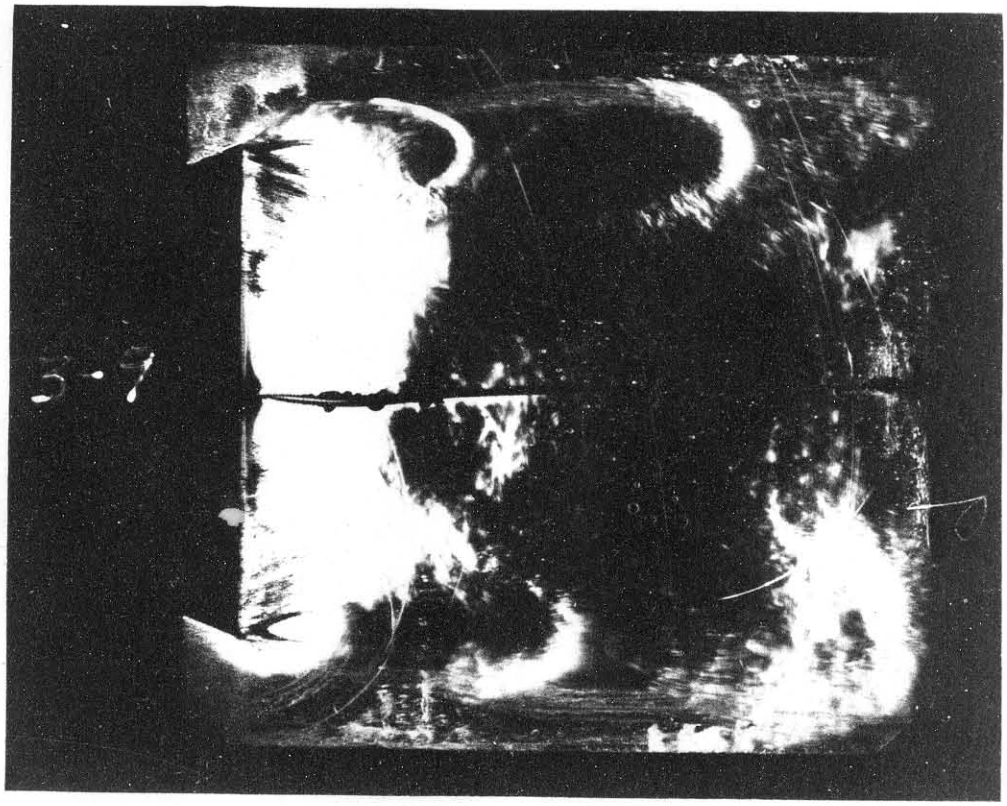

FIGURE 11. TYPICAL FLASH SCHLIEREN PHOTOGRAPHS OF SCREECHING COMBUSTION TAKEN AT THE SAME OPERATING POINT

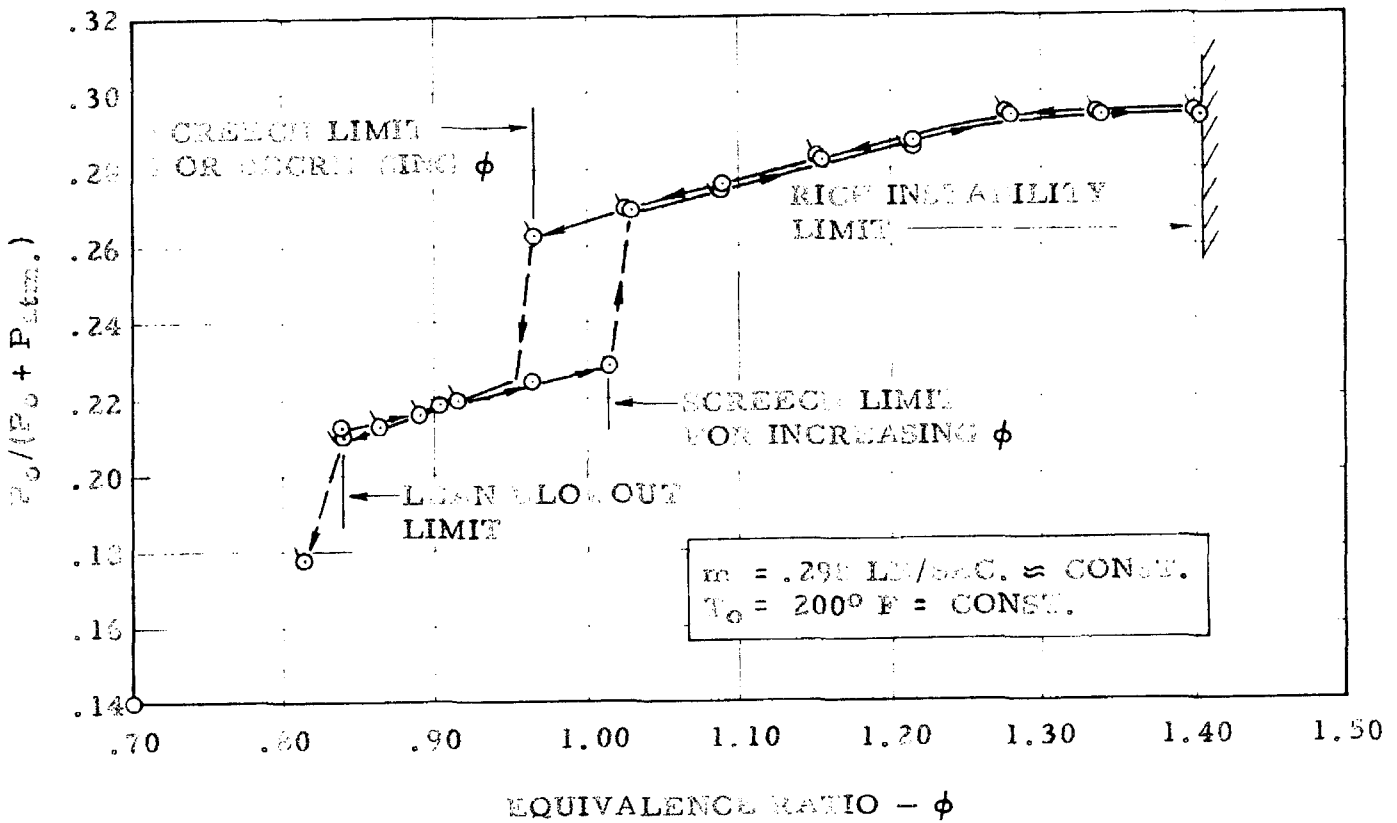

FIGURE 12. VARIATION OF COMBUSTION CHAMBER INLET TOTAL PRESSURE WITH EQUIVALENCE RATIO

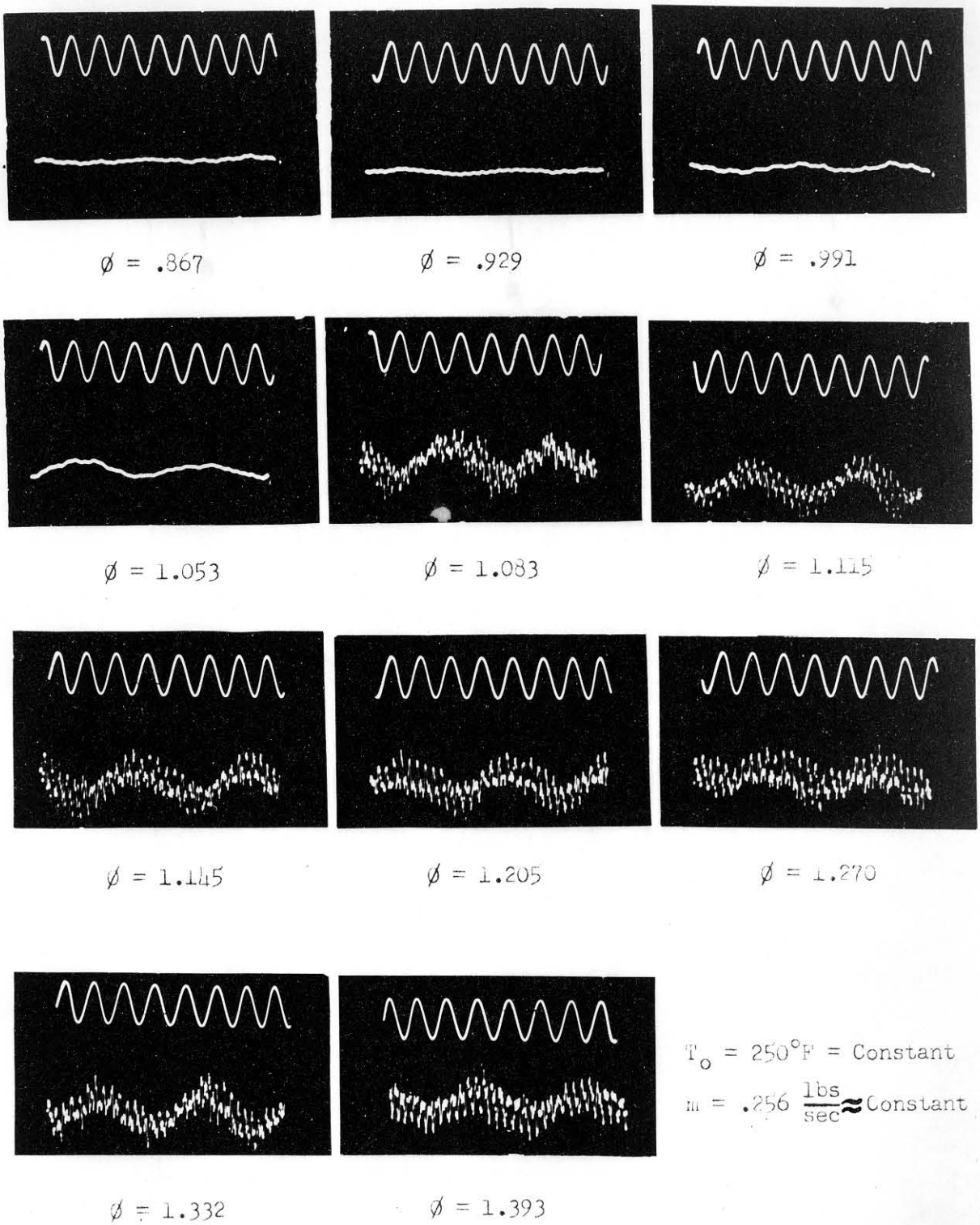

FIGURE 13. TYPICAL PRESSURE TIME TRACES AS A FUNCTION OF EQUIVALENCE RATIO

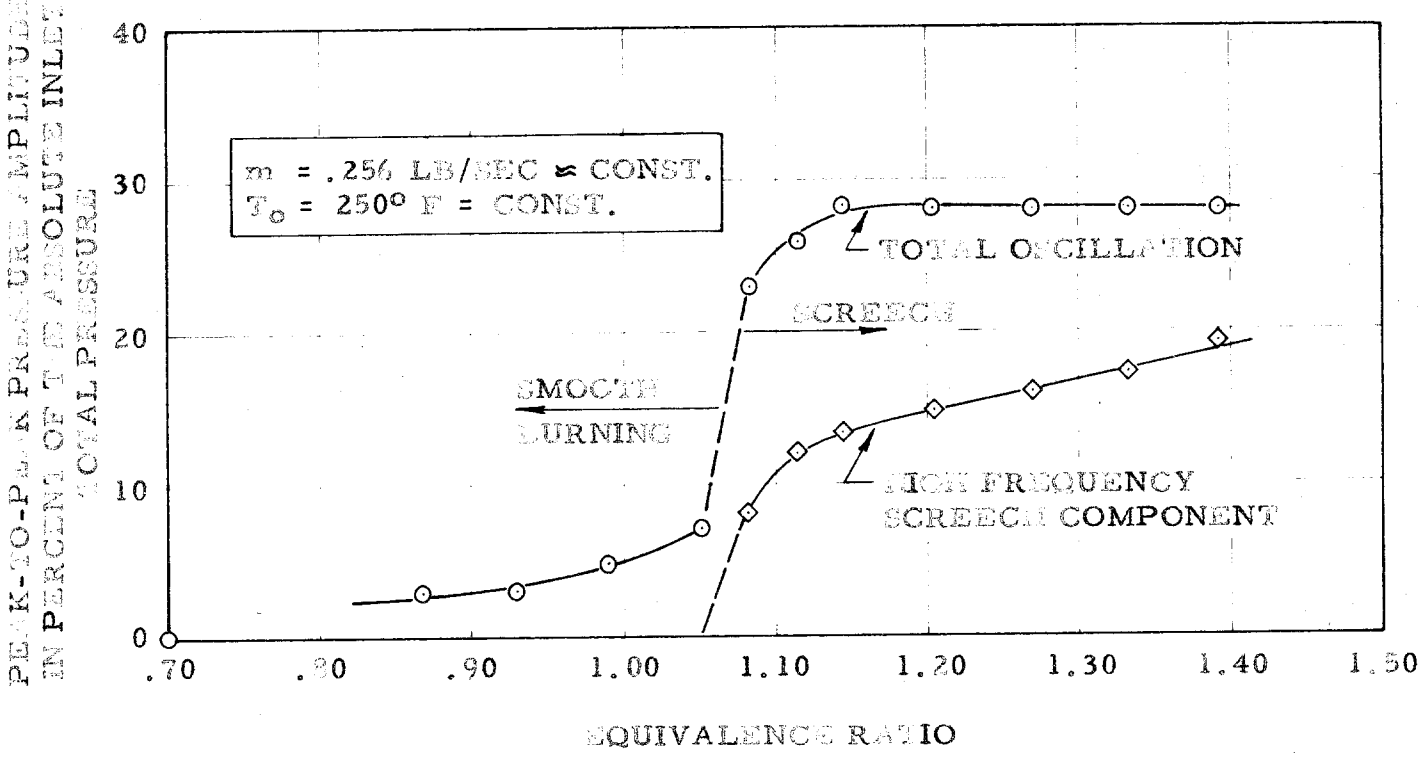

FIGURE 14. VARIATION OF PRESSURE AMPLITUDE WITH EQUIVALENCE RATIO

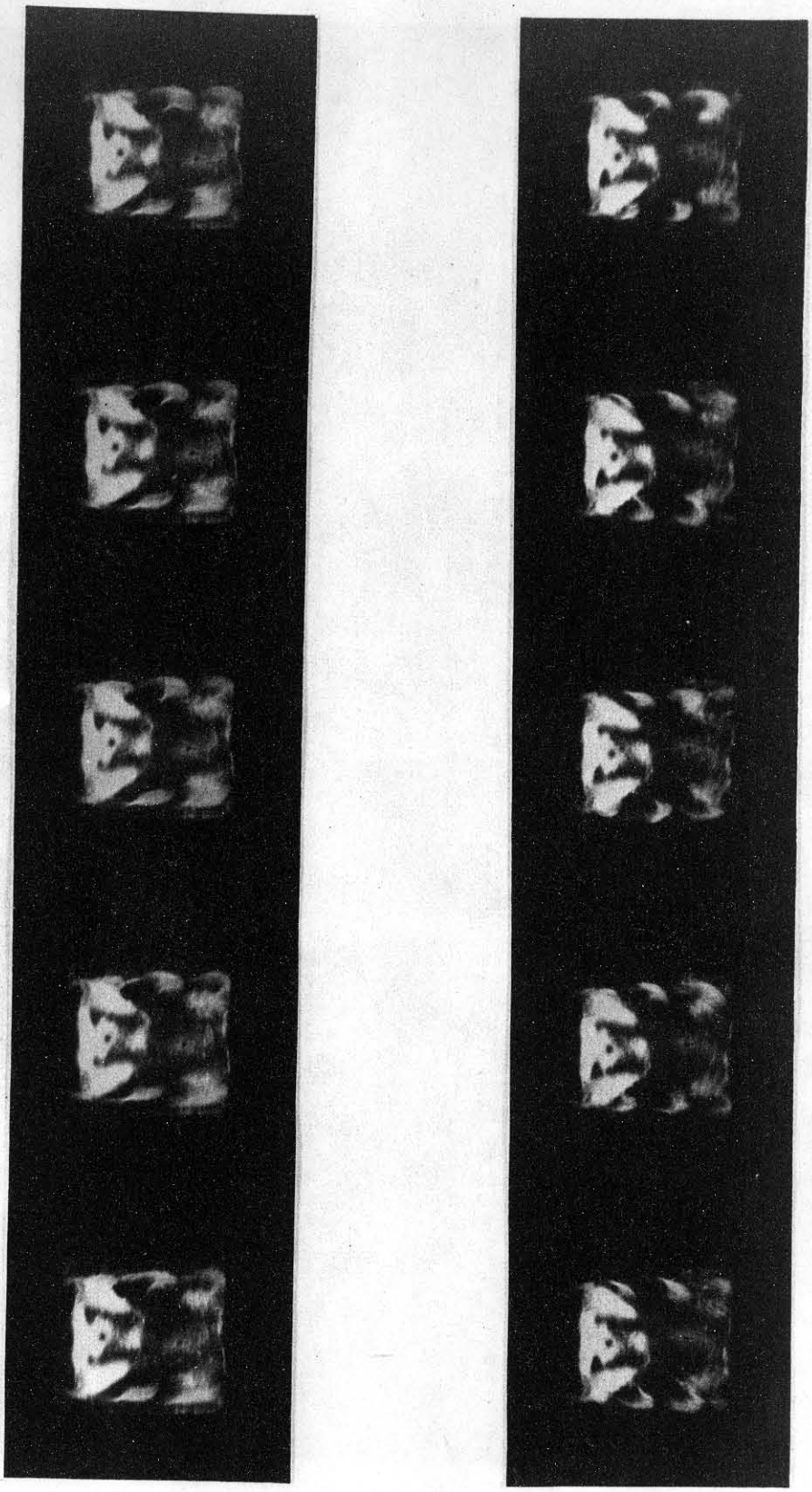

Strip A
4100 Frames/Sec
$\phi = 1.379$

Strip B
7000 Frames/Sec
$\phi = 1.379$

Figure 15 Typical High-Speed Schlieren Moving Pictures of Screeching Combustion

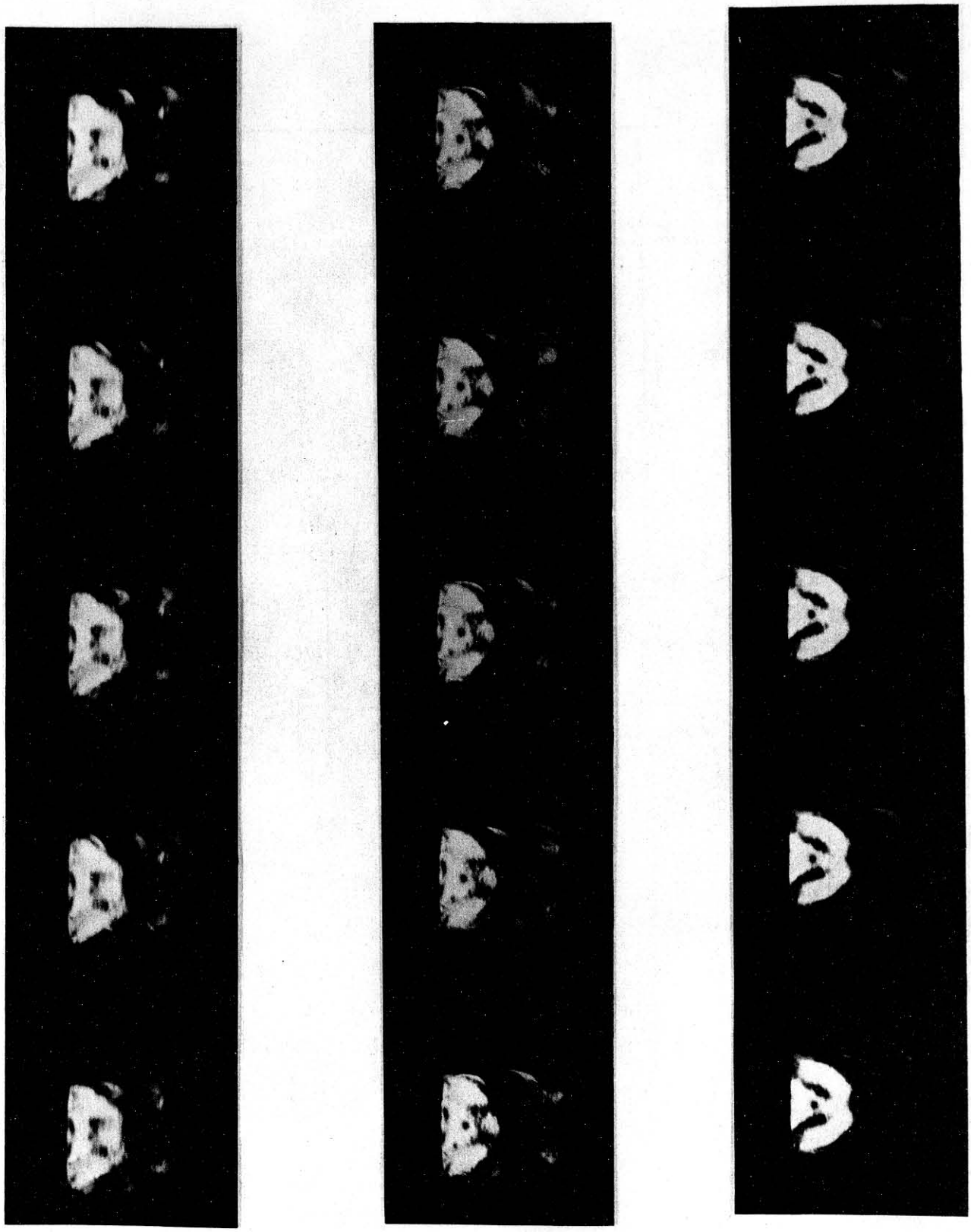

M = .355
Ø = 1.070

M = .432
Ø = 1.055

M = .500
Ø = 1.065

Figure 16 High Speed Schlieren Moving Pictures of Screeching Combustion Showing the Effect of Mach Number on Vortex Formation (7000 Frames per Second)

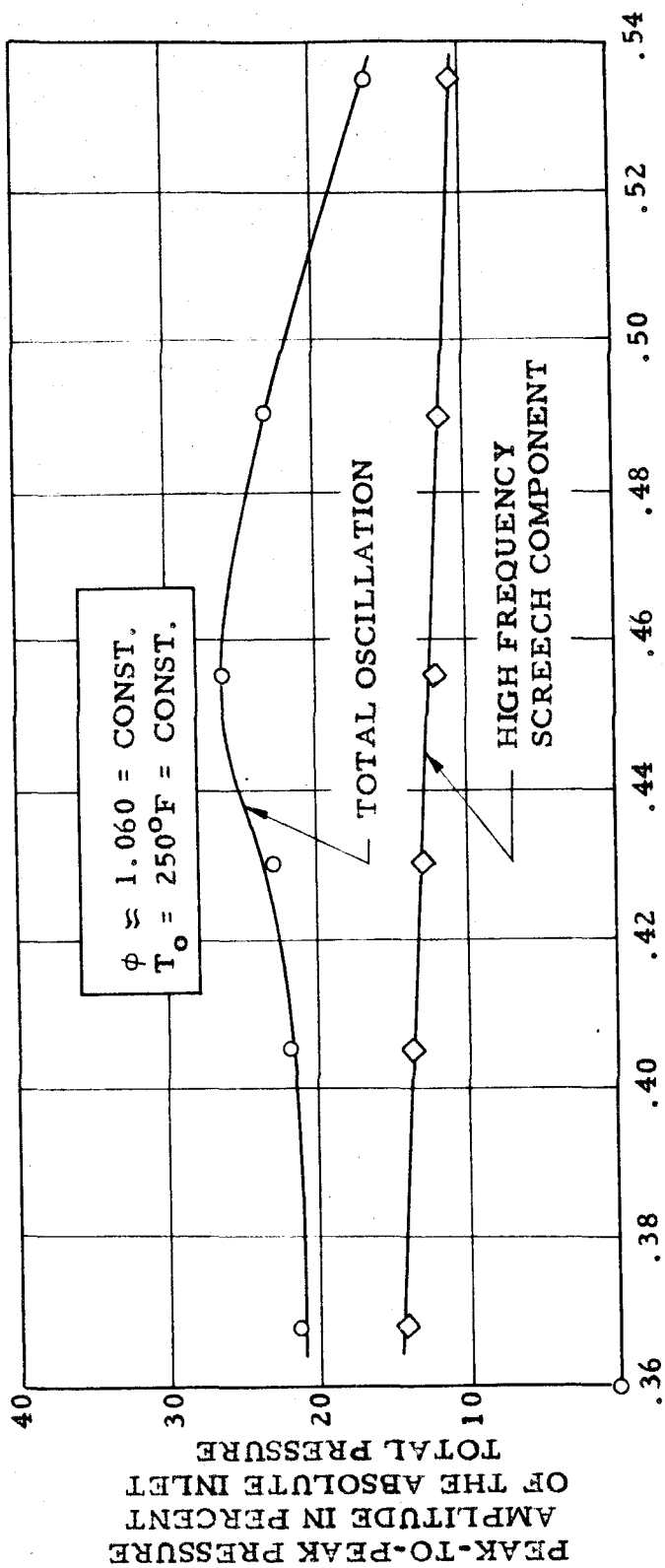

FIGURE 17. VARIATION OF PRESSURE AMPLITUDE WITH THE AVERAGE MACH NUMBER BY THE FLAME HOLDER

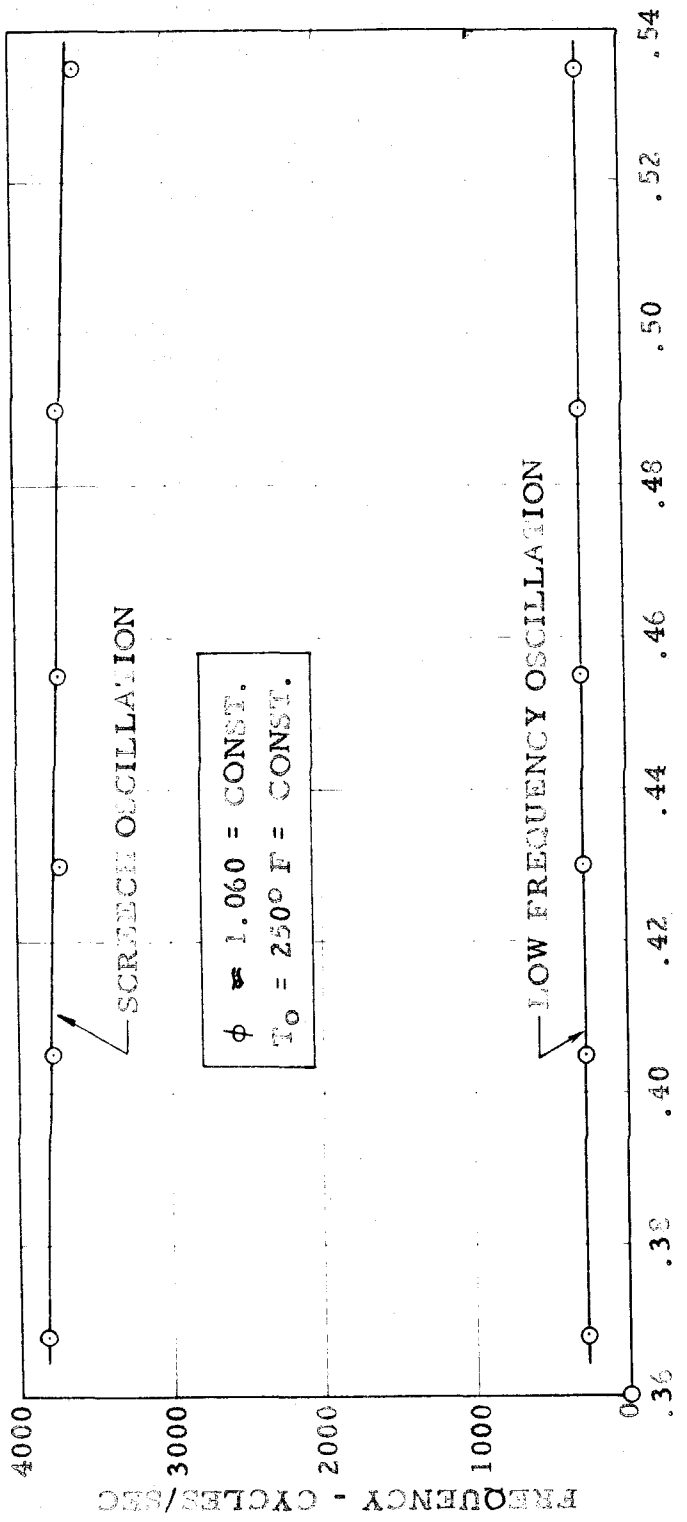

FIGURE 18. VARIATION OF FREQUENCY WITH THE AVERAGE MACH NUMBER BY THE FLAME-HOLDER

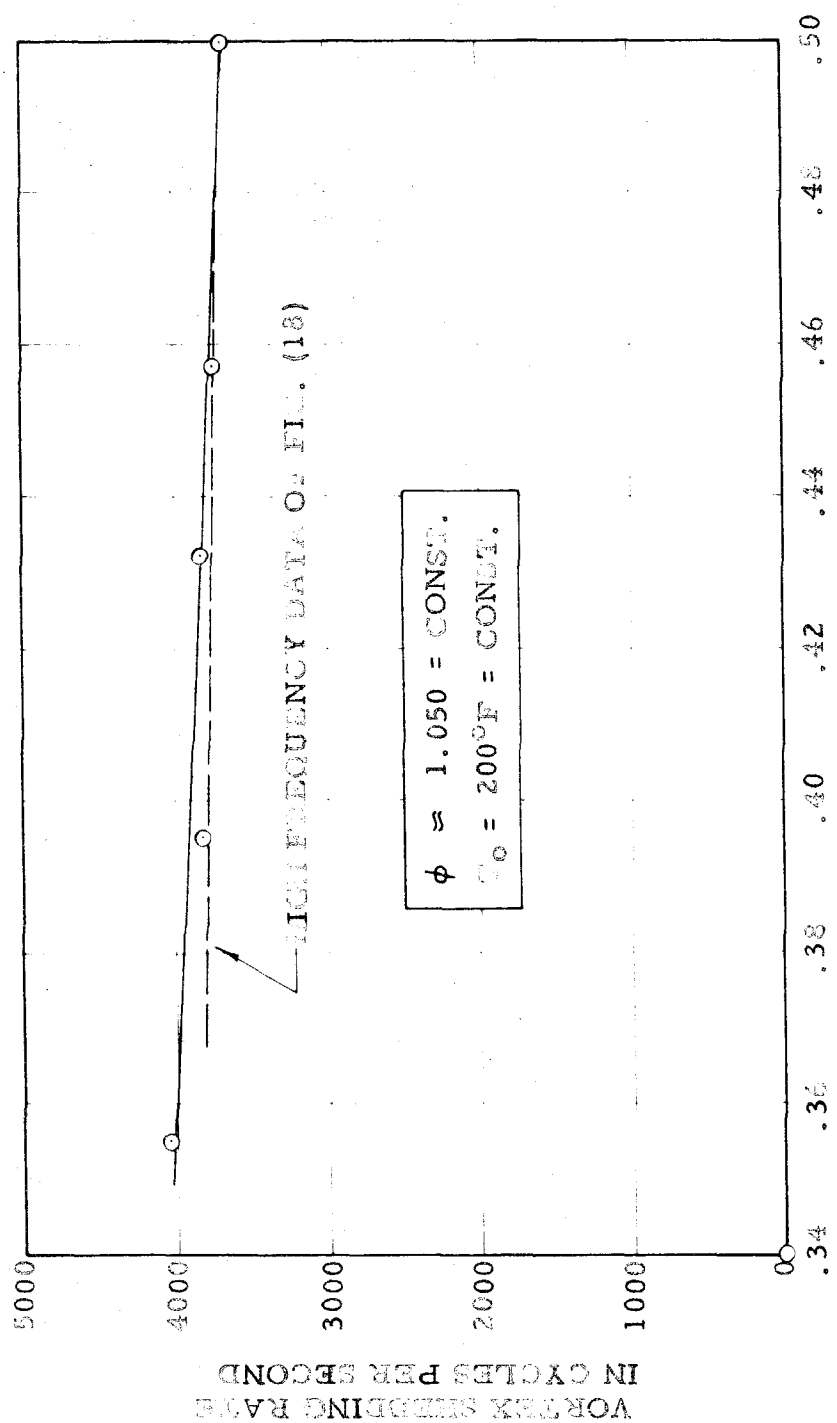

FIGURE 19. VARIATION OF THE VORTEX SHEDDING RATE WITH THE AVERAGE MACH NUMBER BY THE FLAME-HOLDER

FIGURE 20. VARIATION OF THE LEAN SCREECH LIMIT WITH THE AVERAGE MACH NO. BY THE FLAME-HOLDER

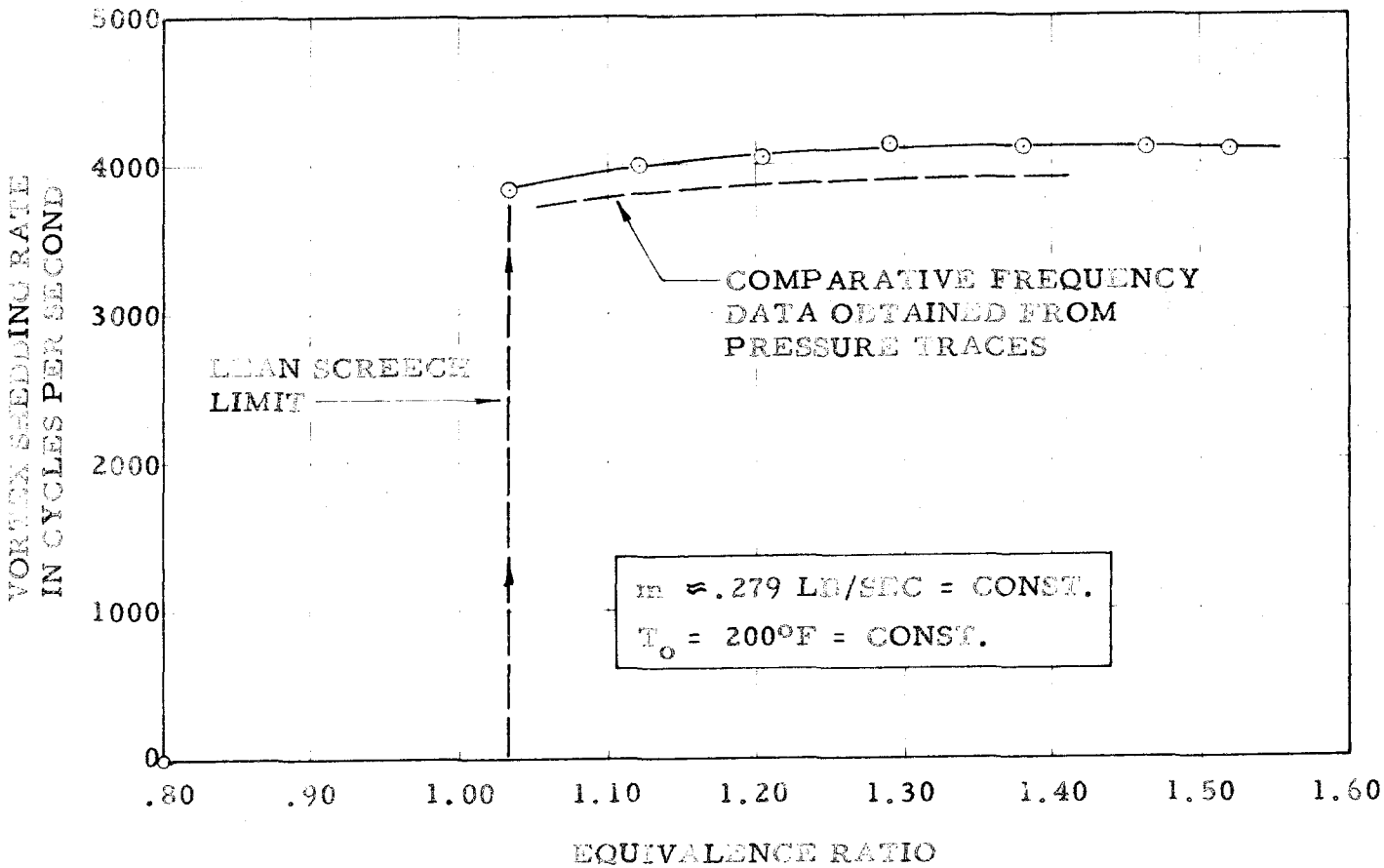

FIGURE 21. VARIATION OF THE VORTEX SHEDDING RATE WITH EQUIVALENCE RATIO

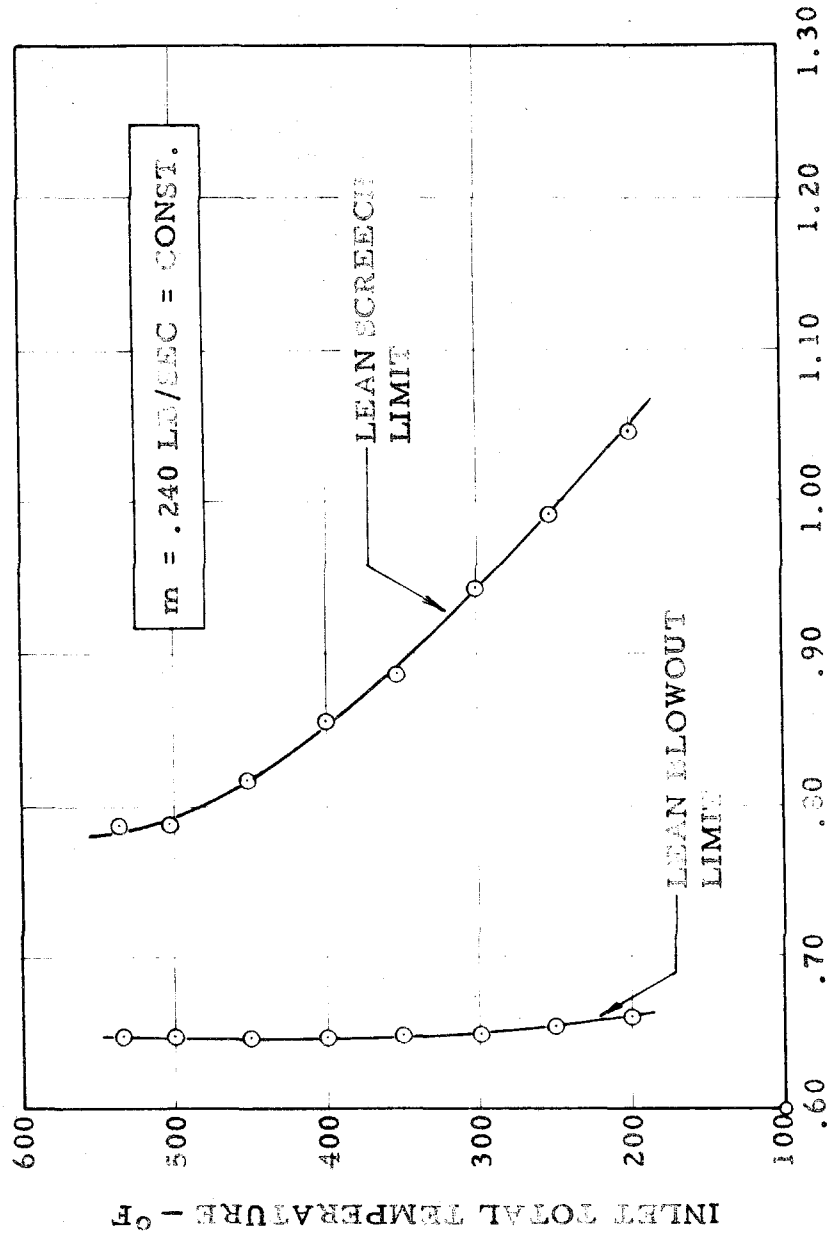

FIGURE 22. VARIATION OF THE LEAN SCREECH LIMIT AND THE LEAN BLOWOUT LIMIT WITH INLET TOTAL TEMPERATURE